Vol. 47, No. 2 (2025) 202-216, DOI: 10.24874/ti.1893.02.25.04

Tribology in Industry

www.tribology.rs

RESEARCH

Wear Patterns on Ball Bearings Lubricated by Grease Contaminated with Several Large Solid Particles

Aidil Ikhsan[a,b], Dedison Gasni[a,*], Meifal Rusli[a]

[a]*Department of Mechanical Engineering, Faculty of Engineering, Universitas Andalas, Kampus Limau Manis, Padang, West Sumatra, Indonesia, 25163,*
[b]*Department of Industrial Engineering, Faculty of Engineering, Universitas Bung Hatta, Jl. Gajah Mada No.19, Gn. Pangilun, Padang, West Sumatra, Indonesia, 25173.*

Keywords:

Ball bearing
Wear mechanism
Solid contaminant
Starvation
Vibration
Temperature
Current

* Corresponding author:

Dedison Gasni
E-mail: dgasni@eng.unand.ac.id

Received: 11 February 2025
Revised: 17 March 2025
Accepted: 9 April 2025

A B S T R A C T

This study aims to investigate the wear patterns due to grease contamination by several types of solid particles on ball bearings. The research was conducted using a ball bearing test apparatus with a load of 300 N with a rotational speed of 2998 rpm for 4 hours. The solid contaminants used were iron sand, coal, silica, limestone, gypsum, and clay with a concentration of 20 wt% and particle sizes of 74 and 250 µm, respectively. During testing, the condition of the bearing and motor was monitored. Wear surface morphology was observed on the inner and outer races of the ball bearing using an optical microscope and SEM/EDX. The test results show that hard contaminants, such as silica and iron sand, predominantly induced abrasive wear through the two-body and third-body wear mechanism, resulting in scuffing and denting. While soft contaminants, such as coal, gypsum, clay, and limestone, primarily caused third-body wear mechanisms with flakes on the surface of the outer ring due to lack of lubricant properties and trigger starvation. SEM/EDX analysis confirms the role of two-body and third-body in accelerating wear progression. Monitoring the vibration, temperature, and current of the bearing and motor could identify the severity of wear.

1. INTRODUCTION

Ball bearings are an important component that is widely used in various applications in various industries, such as the automotive industry, the cement industry, etc. They ensure smooth and efficient machine operation by reducing friction between moving parts. This role is critical to maintaining the reliability and longevity of mechanical systems, which in turn affects overall performance and maintenance costs. Proper lubrication of ball bearings is essential to minimize friction and wear, thus preventing bearing failure and avoiding costly downtime or expensive repairs. Grease is commonly used as a lubricant for ball bearings because it stays in place and provides a consistent lubricating film. However, under real conditions, grease can be contaminated by particles such as dust, dirt, water, and metal debris. Especially in the cement industry, where dusty

environmental conditions originate from basic cement materials such as clay, silica, limestone, etc., which are a source of solid particles that will contaminate lubricants. This contamination significantly changes the lubricating properties of the grease and can accelerate the wear mechanisms [1-3] and reduce rating life [4] of the bearings.

Contaminated grease and oil lubricants can cause various forms of wear, including abrasive wear, adhesive wear, fatigue wear, and corrosive wear, all of which will reduce the operational life of the bearing. Understanding the specific wear mechanisms caused by various solid contaminants is critical for developing better maintenance practices and improving bearing lubrication designs and strategies [5]. Research on the effects of contaminants has been carried out by several researchers using both experimental and numerical approaches with various particle sizes, types of solid contaminants and with different types of lubricants, both solid and semi-solid. Boucherit et al. [6] has carried out analytical and numerical analysis of the effects of solid contaminants on the effects of the dynamic behavior of journal bearings with a percentage of solid particles in the lubricant of 10, 20, and 40%. Research on solid particles in the lubricant in ball bearings against vibration has been carried out by several researchers with vibration analysis [7,8] and acoustic emission signal [9]. Maru et al. [10] have investigated the effect of solid contaminants on wear and vibration analysis. Dwyer-Joyce [11] tried to compare the analytical study with the exprimental approach to understand the wear mechanism on ball bearings due to hard solid contaminants in lubricants. The mathematical modeling and computer simulation have been conducted by Nikas et al. [12] to investigate the effects of debris particles in sliding/rolling on elastohydrodynamic contacts.

The effects of size, concentration, and hardness of solid particles greatly influence the wear that occurs on the surface and the level of vibration on the ball bearing. Several studies have been carried out by researchers. Koulocheris et al. [2] have carried out research with various particle sizes of 68, 80, 91, and 141 μm with a hardness of 700 and 2000 HV. The results of the research show that the harder the particles are, the greater thw wear will be, and the size effect particles vary depending on particle hardness and brittleness as soft ductile particles are rolled over and hard brittle particles are crushed down. Hariharan and Srinivasan [7] investigated vibration levels with particle sizes of 90, 150, and 300 μm with concentrations of 10, 20, and 30% each. The research results show that there is a significant variation in the RMS velocity values on varying the contaminant concentration and particle size. Ibrahim Sheriff et al. [9] investigated the effect of acoustic emission signals in ball bearings with particle sizes of 75, 106, and 150 μm and concentration levels of 5, 15, and 25%, respectively. The research shows that the trends in the amount of acoustic emission waves are affected by the contamination of the grease. Maru et al. [10] investigated the effect of solid contaminants in liquid lubricant with concentrations of 37, 59, and 111 μm and with concentrations of 0.05, 0.35, and 0.5 g/l, respectively. The results show that the vibration level is different for concentration and particle size, and wear increased with increasing particle concentration. Dwyer-Joyce [11] has predicted the abrasive wear on ball bearings due to solid particles and compared it with the experimental study. The result shows that the abrasive action of each particle is determined by the volume of material displaced during sliding and another empirical factor for the proportion of this removed as a wear particle. According to Nikas et al. [12], the ductile and soft debris particles are responsible for high flash temperatures and destructive sliding contact where the particles tend to accumulate in the inlet zone of contacts, causing fluid starvation.

The type of solid particle can be in the form of debris that comes from wear and tear that occurs on two surfaces in contact and can also be in the form of foreign particles that enter the oil lubricant and solid. The types of solid contaminants used by previous researchers can be steel particles [2], silica [7,13], green sand [9], diamond abrasive particles [11], corundum [4], quartz (SiO_2) [10], and environmental particles [14,15]. Research that systematically investigates the impact of various types of contaminants on ball bearing wear patterns is still limited. Most existing studies focus on the effects of one type of contaminant or general wear behavior without distinguishing between different contaminants. This research aims to fill this gap by providing a comprehensive investigation of the wear patterns of ball bearings lubricated with grease contaminated by various substances found in the cement factory environment. By identifying and understanding different wear patterns of the

outer and inner ring surfaces through surface morphology analysis using SEM/EDX analysis and monitoring of parameters, such as temperature distributions, vibration levels, and current distribution of bearing and motor, respectively, caused by various solid contaminants, this research aims to provide valuable insights to improve bearing performance and reliability in contaminated environments.

2. MATERIALS AND METHODS

2.1 Grease

In this study, semi-solid lubricant was utilized. Top I HI-Temp Grease (NLGI standard) was employed. Produced with synthetic base oils, Top I Hi-Temp grease is a multipurpose lithium complex grease. Table 1 shows the grease's physical properties.

Table 1. Physical Properties of Top I HI-Temp Grease [16].

Properties	Remarks
Grade, NLGI ASTM Test	2
Thickener	Lithium Complex
Texture	Smooth, Tacky
Color	Observed Blue
Viscosity: cSt @ 40°C	538
Worked 60 Penetration D-217	265-295
Dropping Point, ºC D-2265	>260
Water Washout, % loss D-1264	2.5 @ 80ºC
Timken OK Load, lb. D-2509	80
Four-Ball EP Weld Point, kgf D-2596	315
Approximate Temperature Range, °C	-23 to 163
NLGI Classification	GC-LB

2.2 Solid contaminants

The solid contaminants used for this test were obtained from the area around PT Semen Padang, Indonesia, which is the raw material for making cement. Solid contaminants used in this research consisted of coal, silica, gypsum, clay, iron sand, and limestone. Feature of solid contaminants described by particle size and concentration. The concentration of solid contaminants was 1 g from 5 grams of grease, or 20 wt%, and the grain size of solid contaminants was 74 and 250 μm, respectively, which were mixed into the grease. Mixing was done by stirring to ensure the solid contaminant was mixed evenly in the grease. A sieve shaker with mesh sizes of 200 and 60 mesh was used to get the particle size of 74 and 250 μm.

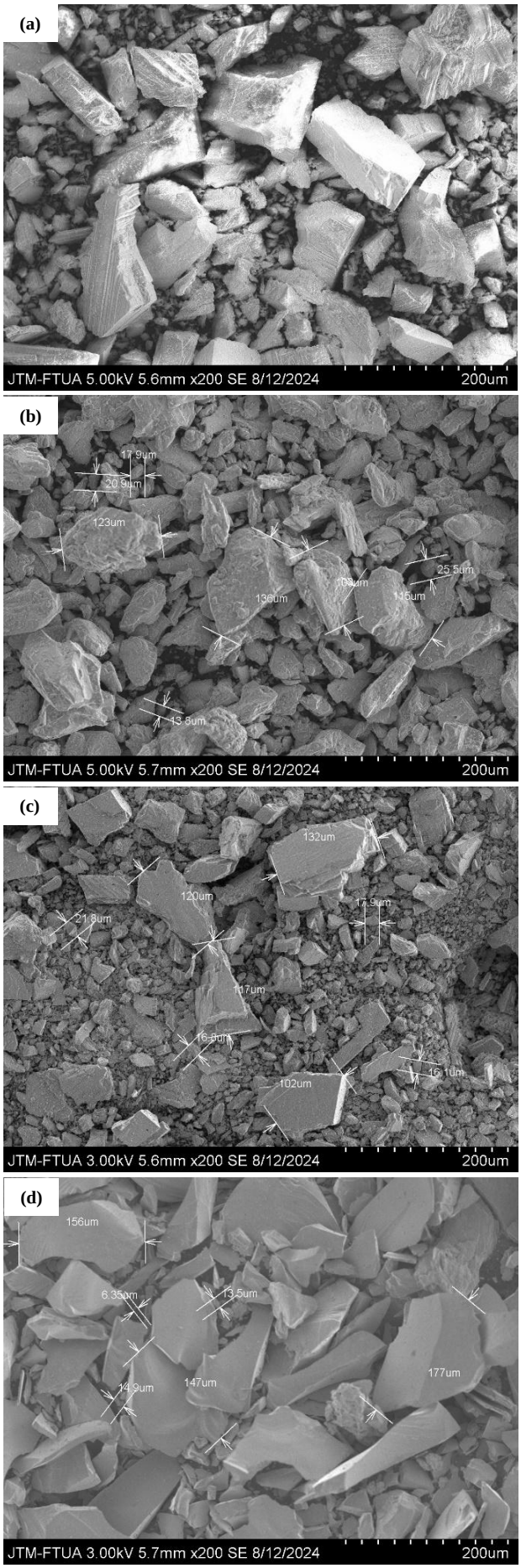

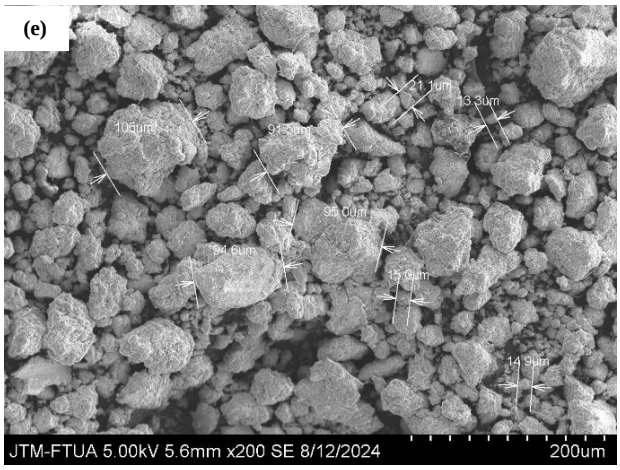

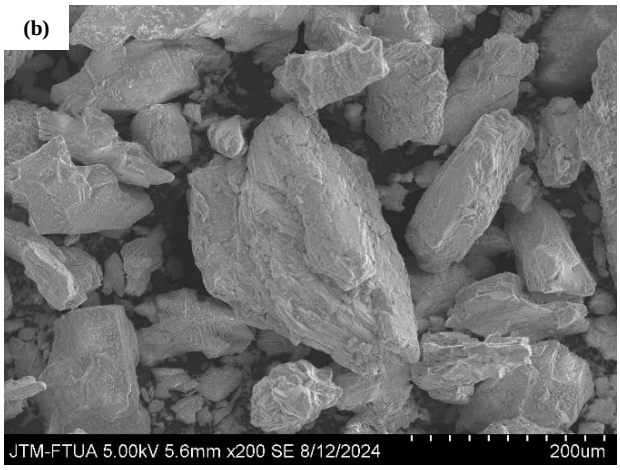

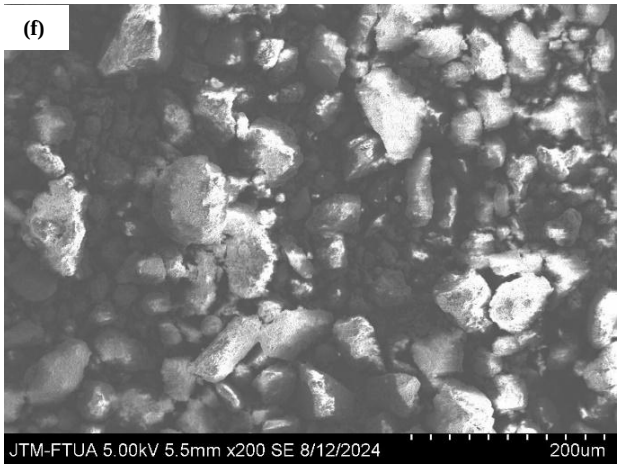

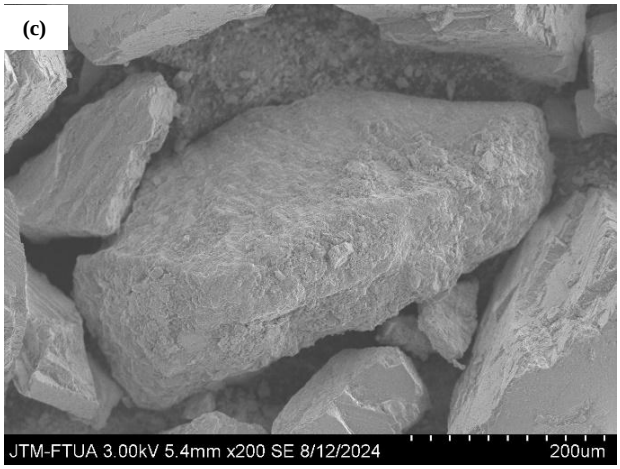

Fig. 1. SEM morphology of 74 μm size of solid particle contaminants used in this study (a) silica, (b) gypsum, (c) limestone, (d) iron sand, (e) clay, and (f) coal.

The particle size examination of all solid contaminants using SEM can be seen in Figs. 1 and 2. From the figures, it can be seen that the particle size for small sizes varies, starting from very small sizes to the largest size of 75 μm (Fig. 1), as well as the size of large solid contaminants, starting from small <75 μm to the largest size of up to 250 μm (Fig. 2). The shape of solid contaminants varies from round particle shapes, round with spherical shape edges, long round, long with squares, and long flat.

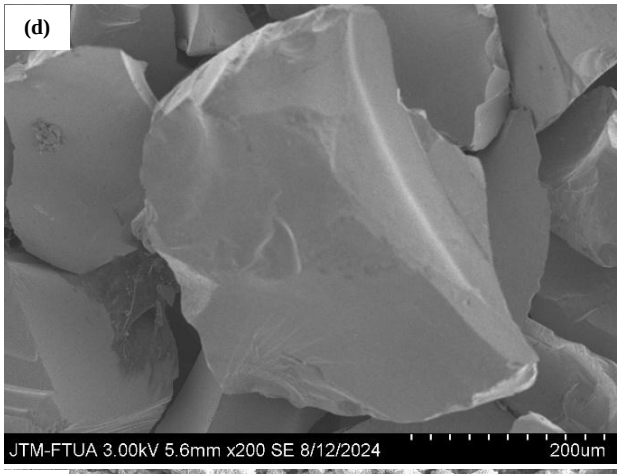

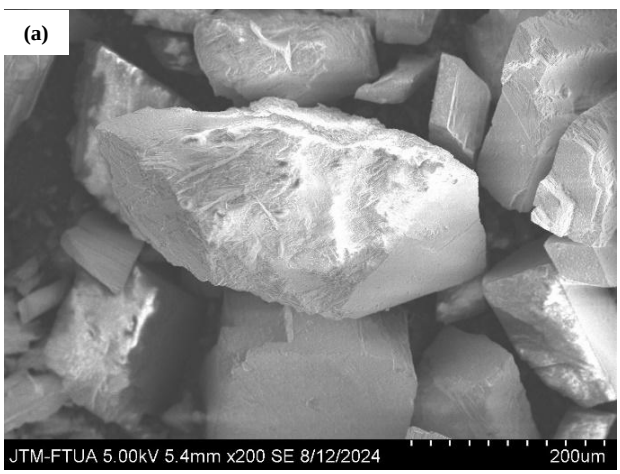

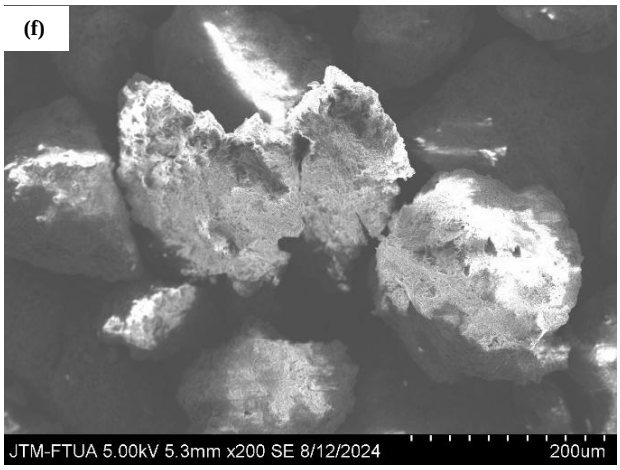

Fig. 2. SEM morphology of 250 μm size of solid particle contaminants used in this study (a) silica, (b) gypsum, (c) limestone, (d) iron sand, (e) clay, and (f) coal.

2.3 Ball bearings

The ball bearing used was a single-row, deep-groove ball bearing manufactured by ASB with type 6206 2RS, which is sealed on both sides, adhering to a flat surface of the inner ring. The geometry of the ball bearings tested can be seen in Fig. 3, and the geometric properties of the ball bearings can be seen in Table 2.

Table 2. Geometrical properties of ball bearing (6206).

Property	Value (mm)
Bearing outside diameter, *D*	62
Bearing bore diameter, *d*	30
Bearing width, *B*	16
Ball diameter, BD	9.65
Contact angle, *β*	0
Number of balls, *n*	9

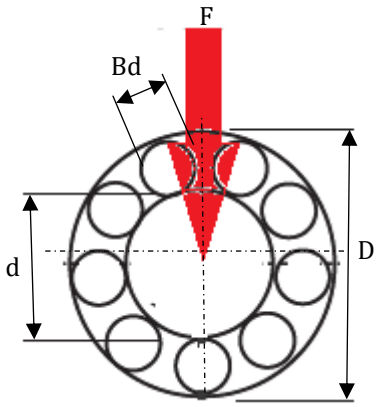

Fig. 3. Geometry of the ball bearing (6206).

2.4 Experimental setup

Ball bearing test equipment is made as shown in Fig. 4, which aims to measure the wear, temperature, vibration levels that occurred in ball bearings, and the current of the motor. This equipment consists of a motor with a power of 1.5 hp and a rotational speed of 2998 rpm. Power from the motor is transmitted to the supported shaft using ball bearings at both ends, and contaminated ball bearings are installed in the middle using a belt transmission system with a 1:1 ratio. The type 6206 ball bearing used for analysis was installed on a shaft size of 30 mm in a rigid housing so that the inner ring rotates. A radial load of 300 N was applied to the bearing by a simple rod mechanism with a load of 10 kg. Accelerometer and thermocouple sensors were installed on the bearing to obtain the vibration and temperature levels that occur while the bearing is working. The current of the motor was measured by using a PZEM-004T V2.0. It can measure the current 0 ~ 100 A and working voltage 80 ~ 260 VAC. All signals from the accelerometer, thermocouple, and current meter were transferred to the PC using data acquisition (DAQ). Type K thermocouples were used to measure the temperature on the bearings, where this thermocouple is capable of measuring temperatures in the range of 0°C - 800°C with an accuracy of up to 0.25°C with a working voltage of 3 - 5 V. Vibration signatures were analyzed in terms of root mean square (RMS) values.

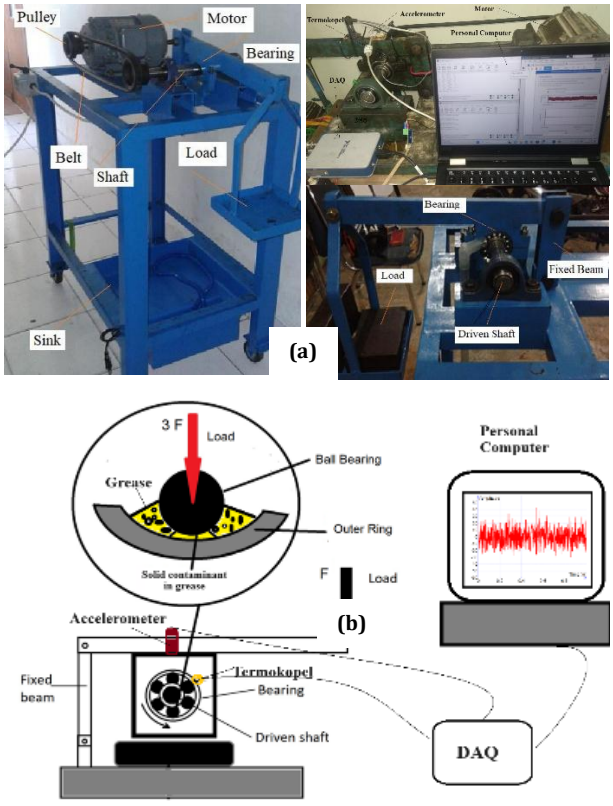

Fig. 4. (a) Ball bearing apparatus and (b) schematic diagram of ball bearing apparatus.

2.5 Procedures

Before solid contaminants were used, they were examined to investigate their shape and size of the solid contaminant as shown in Fig. 1. All ball bearings that have been lubricated with 6 types of contaminants mixed with grease were installed in the test equipment as in Fig. 4. Measuring was carried out for 4 hours for each different type of solid contaminant. Vibration, temperature, and current data were captured during measuring. After the test was complete, the wear that occurred on the surface of the inner race and outer race of the ball bearing itself was examined using an optical microscope, SEM, and energy dispersive X-ray (EDX).

3. RESULTS

3.1 Monitoring condition of bearing and motor

RMS amplitude vibration measurement of bearing

Vibration measurement used an accelerometer mounted on a bearing housing in the radial direction along the vertical axis. The root mean square (RMS) amplitude measured on an accelerometer whose data was read for 4 hours with variations in solid contaminants and particle sizes can be seen in Figs. 5 and 6.

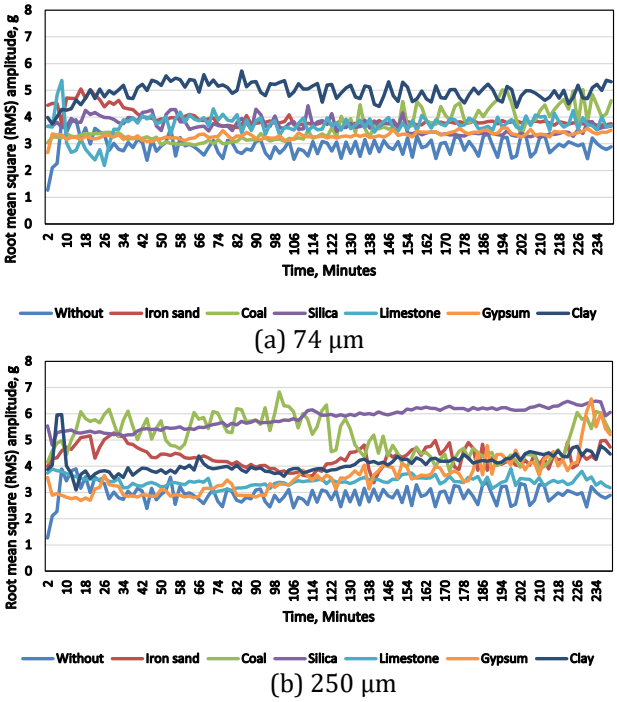

Fig. 5. RMS amplitude vibration for different solid contaminants with a particle size of (a) 74 µm and (b) 250 µm.

The RMS amplitude of without contaminant was used as comparison. From Fig. 5, in general, it can be seen that the particle size would influence the RMS amplitude vibration when compared to the RMS amplitude without contaminants.

The larger the particle size, the greater the average RMS amplitude vibration that occurred, except for particle sizes of limestone and clay, as shown in Figure 6. However, the influence of the type of solid contaminant on the magnitude of the vibration amplitude that occurs was different for the type of particle size. In general, the RMS amplitude vibration that occurs for various solid contaminants would experience a low RMS amplitude vibration at the beginning, then increase, then tend to fluctuate, decrease, and then remain stable. The differences in RMS amplitude vibration among solid particles were varied, where small particle sizes provided a wider band RMS amplitude vibration compared to large particles. At a particle size of 74 µm, clay solid contaminant provided the largest RMS amplitude vibration, while at a 250 µm particle size, silica and coal solid contaminants provided the maximum vibration amplitude. It is interesting to see (Fig. 5b) that the coal solid contaminant at a particle size of 250 µm had RMS amplitude vibration increased and fluctuated against time and reached the maximum value at around 102 minutes, then decreased dramatically and increased again at 222 minutes. Different case with gypsum solid contaminant with a particle size of 250 µm: at the beginning, RMS amplitude vibration was low and then increased continuously until at 232 minutes, reaching maximum value.

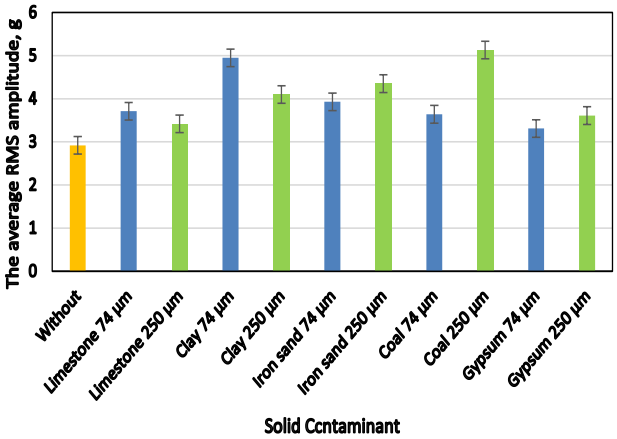

Fig. 6. Comparison of the average RMS amplitude for two solid particle sizes of 74 and 250 µm.

Temperature measurement of bearing

Fig. 7 shows the results of temperature measurements using a thermocouple sensor mounted on the ball bearing for various types of solid contaminants and particle sizes with temperature of bearings without contaminant in grease. From the figure, it shows that the lowest temperature occured without contaminant and the particle size of 74 μm would give a high temperature compared to a large particle size of 250 μm for coal and limestone solid contaminants.

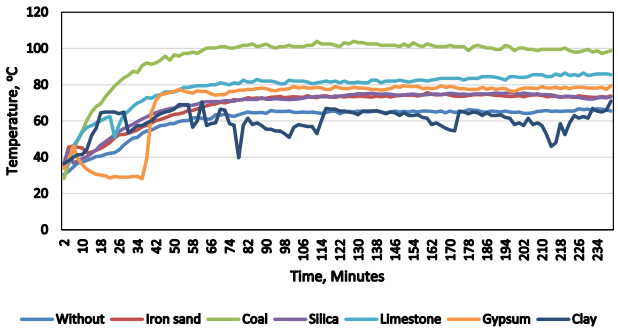

(a) 74 μm

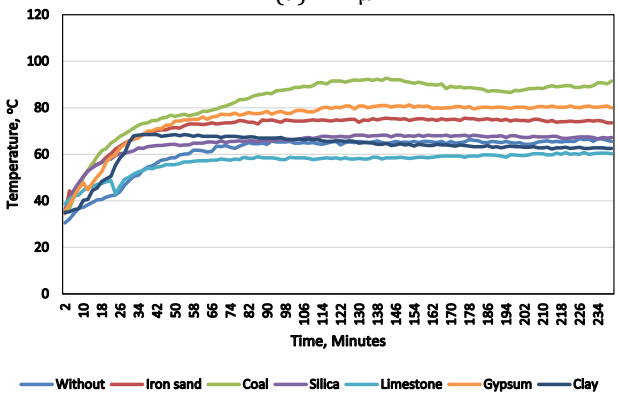

(b) 250 μm

Fig. 7. Temperature of ball bearing for different solid contaminants with particle size of (a) 74 μm and (b) 250 μm.

The temperature of the ball bearing due to several solid contaminants and particle sizes in the grease would increase as time increases. In general, it can be seen that there was a drastic increase in temperature at the beginning of ball bearing running and then tended to stabilize in the following minutes. For both particle sizes, the temperature rise of the ball bearing would vary depending on the types of solid contaminants, where the lowest temperature of the bearing for the particle sizes of 74 and 250 μm was clay and limestone, respectively. The decrease in temperature during gypsum testing (Fig. 7a) is thought to occur due to proper lubrication in the contact area; as time passes, solid particles will accumulate in the inlet contact area, resulting in a lack of lubrication, high friction, and an increase in temperature. Coal solid contaminant gave the highest temperature ball bearing among solid contaminants for both particle sizes, and the highest temperature was reached at around 100°C at a particle size of 74 μm (Fig. 7a).

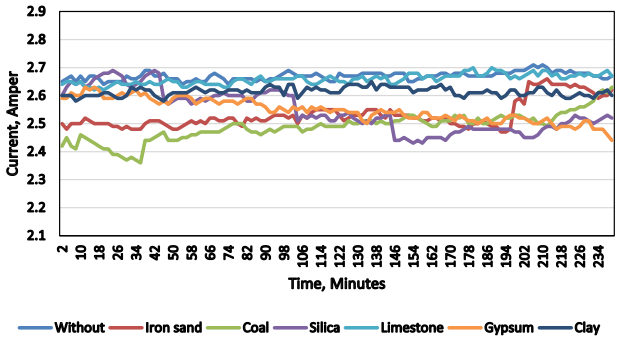

(a) 74 μm

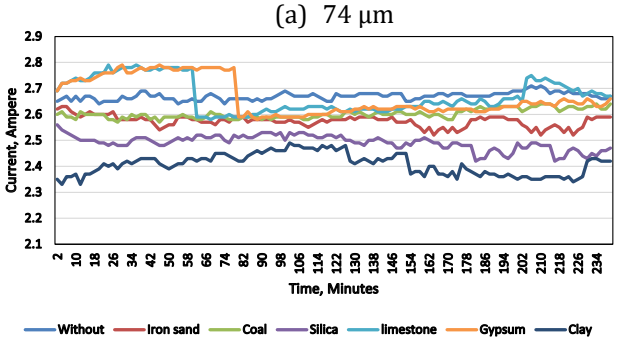

(b) 250 μm

Fig. 8. Current of motor for different solid contaminants with a particle size of (a) 74 μm and (b) 250 μm.

Current measurement of motor

The amount of motor torque used during bearing testing for various types of contaminants and particle sizes in the grease was measured indirectly by installing an amper sensor to measure the amount of current used by the motor. The results of measuring the current used by the motor during testing with variations in solid contamination and particle size can be seen in Fig. 8. From this figure, it can be seen that the current used during testing fluctuated, but some of them tended to be constant, increased, and decreased.

The current of bearing without contaminant has an above-average value of solid contaminants. For both types of particle sizes, limestone solid particles provide the largest current among

solid particles, where the current fluctuates and tends to be constant at a particle size of 74 µm. At a particle size of 250 µm, limestone and iron sand at the beginning of the test gave a high current, and at 72 and 92 minutes, the current tended to decrease for these two types of solid particles (Fig. 8b). The current of the motor lubricated by silica and gypsum solid particles tends to increase in the beginning, and as time goes by, it tends to decrease, in contrast with coal solid particles, as shown in Fig. 8a). The lowest current was recorded on clay solid particles at a particle size of 250 µm, where it was increased in the beginning and then decreased as time increased.

3.2 Wear scar of outer and inner races

Ball bearing equipment has been used to investigate the wear that occurs on the ball bearings diluted with grease that has been contaminated with several types and sizes of solid contaminations. The measurement was carried out for 4 hours with a load of 300 N, and after testing, the inner ring and outer ring were cut, where at the outer ring the lower side was cut and examined due to maximum wear reflecting the higher dynamic forces concentrated on the outer race due to the rotating inner race [17].

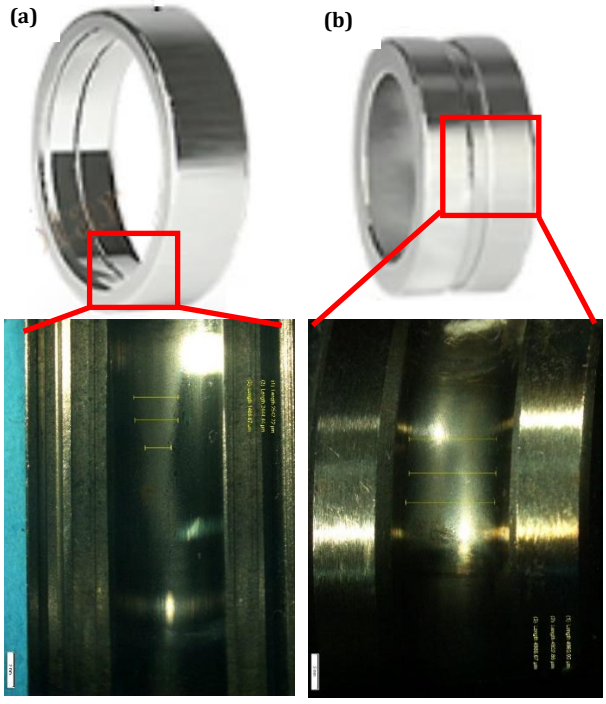

Fig. 9. Photos of wear scar of (a) outer race and (b) inner race.

In general, the wear that occurs on the ball bearing was observed using an optical microscope as shown in Fig. 9. From the observation results of Fig. 9a, it shows that the wear that occurred on the outer ring was not uniform, where the width of the scar on the lower side was wider than that of the upper side. Meanwhile, the wear that occurred on the inner race was uniform on all sides for all solid contaminants.

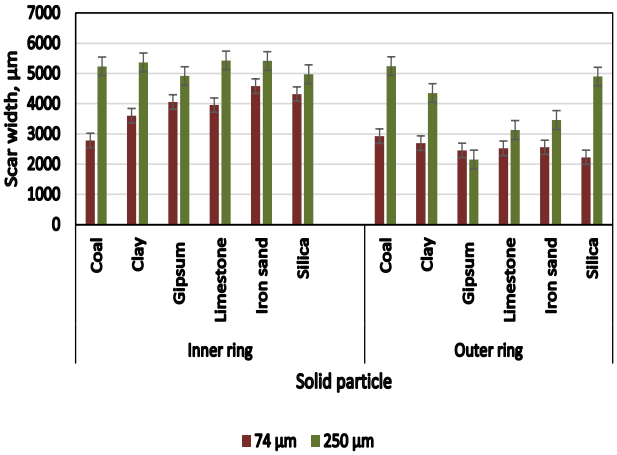

Fig. 10. Comparison of scar width of the inner and outer races with different solid contaminants and particle sizes.

The results of measuring wear scars on the inner and outer races with a variety of solid contaminants using an optical microscope can be seen in Fig. 10. From this image, in general, it can be seen that for several variations of solid contaminants, the scar width of the inner race was greater than the scar width of the outer race. Likewise, the influence of the size of the solid contaminant: the larger the particle size, the greater the scar width of the inner and outer races except for gypsum at the outer race. The largest scar width that occurs in the inner race for the two largest types of particles was caused by solid particle iron sand solid contaminant. Meanwhile, on the outer race, the largest scar width was caused by coal solid contaminant.

3.3 Surface morphology analysis using SEM and EDX

Figs. 11 and 12 show the wear surface morphology of the outer race from SEM images, magnified by 1000, caused by various solid contaminants in grease particle sizes. The

particles have sizes of 74 and 250 μm, respectively, a load of 300 N, and a rotational speed of 2998 rpm for four hours. Each solid contaminant had a distinct wear mechanism caused by solid particles. It is shown by these SEM images that the wear on the outer race's surface increases with particle size. The surface morphology of the outer race surface caused by iron sand and silica solid particles is shown in Figs. 11a, 11c, 12a, and 12c.

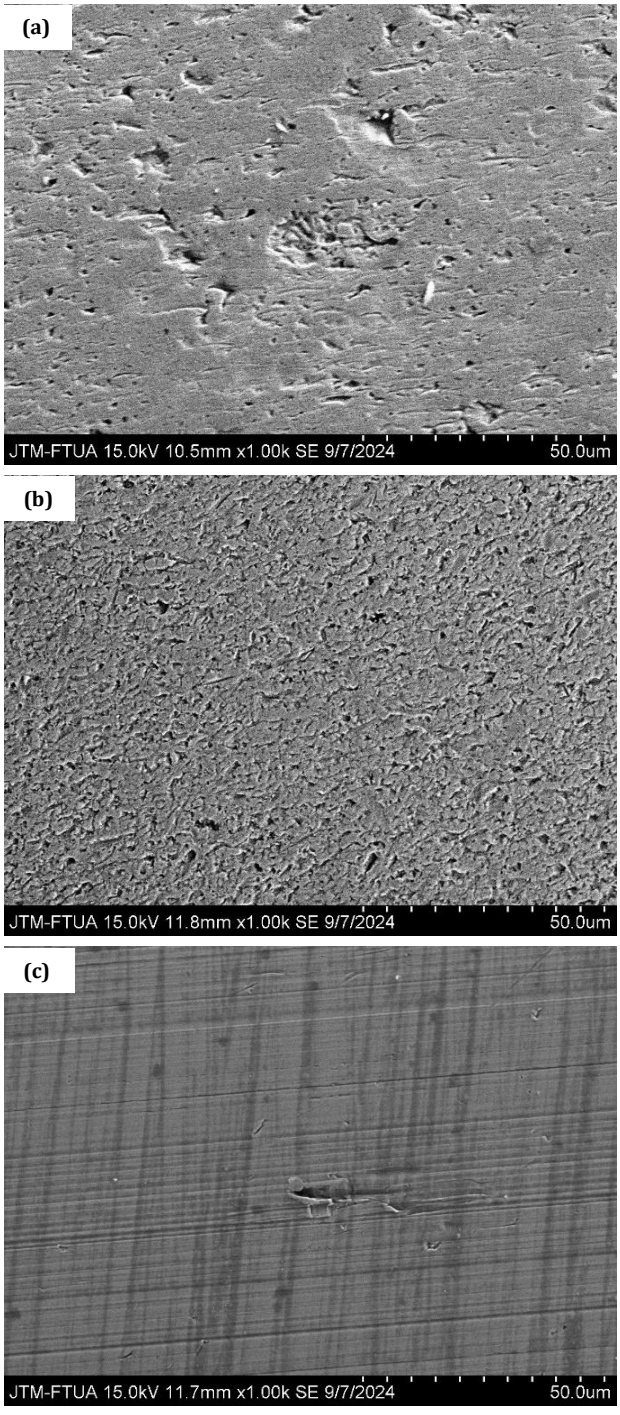

Fig. 11. Surface morphology of the outer race for a particle size of 74 μm with (a) iron sand, (b) coal, (c) silica, (d) limestone, (e) gypsum, and (f) clay solid contaminants.

Abrasive wear was the mechanism of wear, as indicated by scratches and dents on the outer race's surface, which increased in the amount as the particle size rose. The outer race's surface morphology indicates that there are some flakes present on the surfaces of coal solid contaminants with both particle sizes. The absence of lubrication or starvation in the contact

area was found to be the cause of fatigue wear on the surface of the outer race. As the particle size increased to 250 μm, the bearing's temperature rose, as indicated by surface burden on the outer race's surface (Fig. 12b). The similar thing happened to solid particles of clay, gypsum, and limestone; some flakes formed on the outer race's surface, and the number of flakes grew as the particle size increased.

The wear mechanism that occurs due to the presence of solid particles on the surface of the outer and inner races can be abrasive wear, adhesive wear, and fatigue wear. Due to adhesive wear, some material of the ball will stick and material of solid contaminants will stick to the surface of the inner and outer races. Fig. 13 shows the results of EDX analysis, which can be used to study the elemental composition of materials on the surface of the outer race for various types of solid contaminants with a particle size of 250 μm. In general, the main elemental composition of materials of the outer race surface due to being lubricated with various solid contaminants is Fe, O, and C, and another elemental composition is Cr, as shown in Fig. 13. As in the comparison in Fig. 13, the elemental process of the material surface of the outer race before testing was Fe, Cr, and C, and it is indicated that the material of the outer race is high-carbon chromium steel. From EDX analysis, the elemental composition of materials on the surface of the outer race after and before testing by lubricated solid contaminants was different, where after testing, the elemental composition of materials was not only Fe, Cr, and C but also O, as shown in Fig. 14. It is indicated that some elemental composition of contaminant solid material and ball bearing adheres to the surface of the outer race.

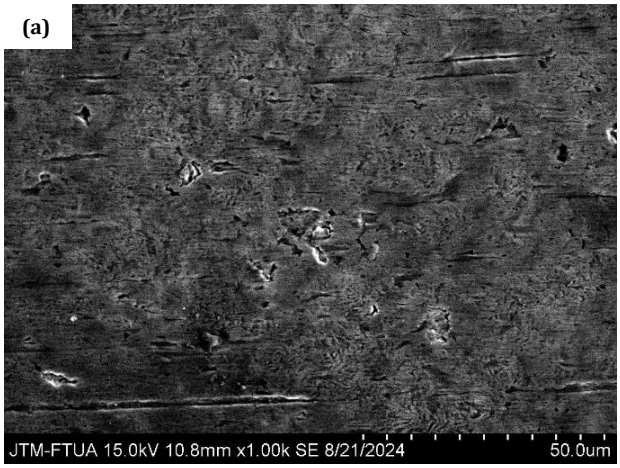

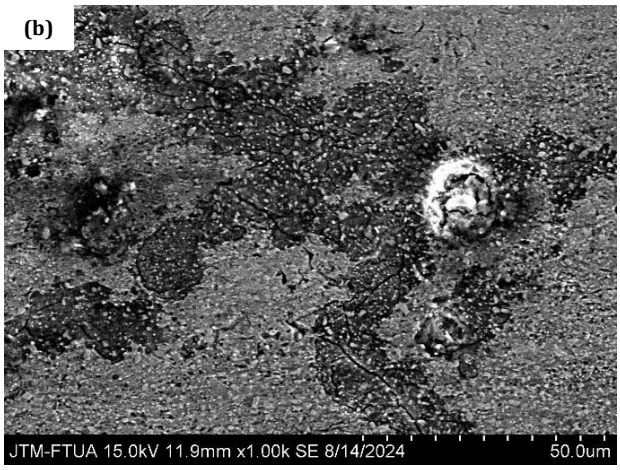

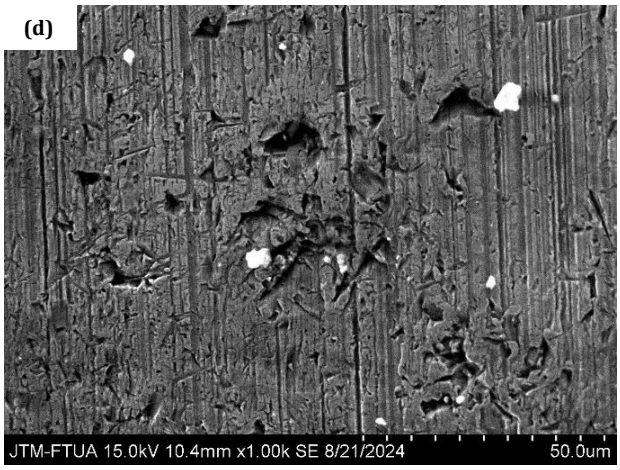

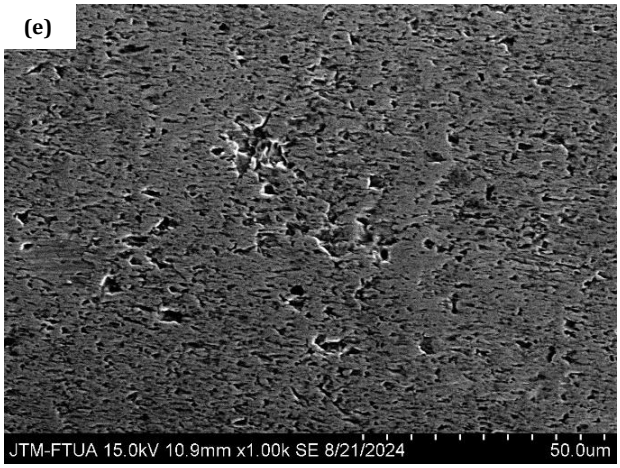

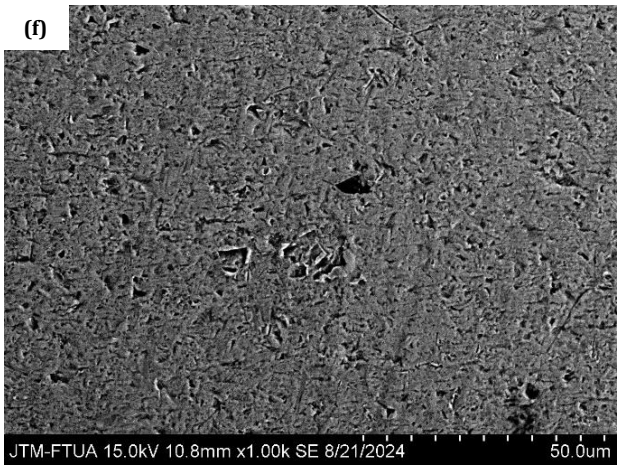

Fig. 12. Surface morphology of the outer race for a particle size of 250 μm with (a) iron sand, (b) coal, (c) silica, (d) limestone, (e) gypsum, and (f) clay solid contaminants.

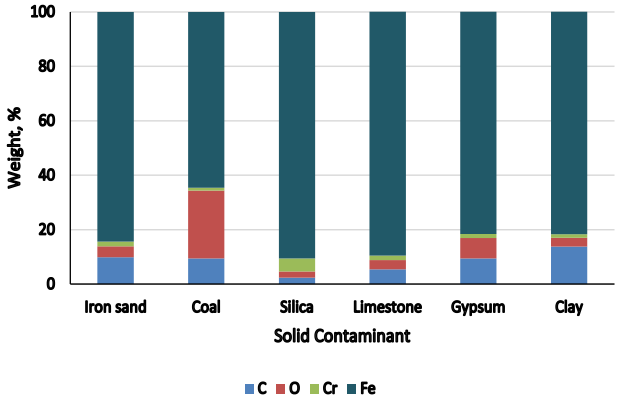

Fig. 13. EDX analysis of surface morphology of the outer ring with different solid contaminants for a particle size of 250 μm.

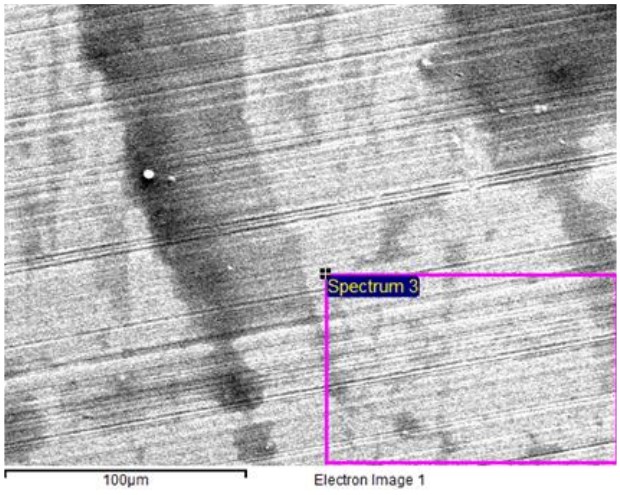

Element	Weight%	Atomic%
C K	11.31	37.18
Cr K	1.74	1.32
Fe K	86.96	61.50
Totals	100.00	

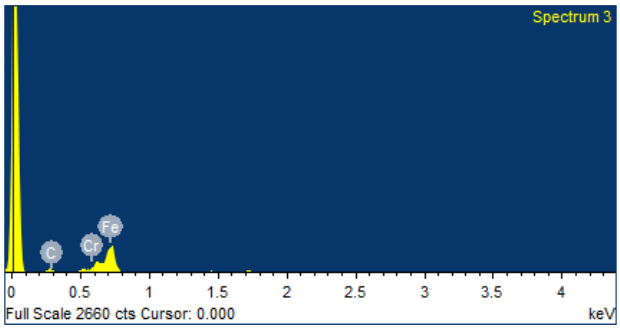

Fig. 14. EDX analysis of surface morphology of the elemental composition of the origin surface of the outer race before testing.

4. DISCUSSION

The investigation into the wear patterns in ball bearings lubricated with grease contaminated by several solid particles provides significant insights into the relationship between contaminant properties, vibration, temperature, current, and surface condition. The findings are discussed below, integrating the concepts of abrasive, adhesive, and fatigue wear to better explain the observed phenomena.

4.1 Influence of solid contaminant properties on wear patterns by using SEM and EDX analysis

In Figs. 1 and 2, it can be seen that from the six types of solid particles with varying particle shapes and sizes (74 and 250 μm). The size variation of all 74 μm particles is in the range of 0 < particle size ≤ 74 μm, while the size variation of 250 μm particles is in the range of 74 μm < particle size ≤ 250 μm. Silica and iron sand are hard solid particles that have hardnesses of 7 and 5.5 Mohs, respectively, while for other solid particles, their hardness is <3 Mohs categorized as soft solid particles [18,19]. When these solid particles enter the contact area, due to very high pressure (3-5 GPa), the ductile and brittle particles are rolled into platelets and crushed into fragments, respectively [11]. The size of the particles will experience a reduction in dimensions. Hard particles that have dimensions larger than the film thickness in the contact area will be pushed out of contact, while particle sizes that are smaller or equal to the film thickness in the contact area will cause third-body and two-body abrasions, but for soft particle sizes, they will experience third-body abrasives where some particles roll over in the

contact area. The abrasive wear that occurs depends not only on the hardness of the particle but also on the shape of the solid particle, such as silica and iron sand solid particles, which have hard particles (>5.5 Mohs) compared to other particles. The shapes of silica and iron sand solid contaminants are long, round, and flat, respectively. From SEM analysis, it seems that the hard contaminants, such as silica and iron sand, induce scratches and dents due to abrasive wear, a phenomenon well-documented in tribology studies highlighting the abrasive effects of hard two-body and third-body particles (e.g., Hamilton et al. [5]), which is a hallmark of two-body and third-body wear. These contaminants act as two-body and third-body, penetrating the lubricant film and directly interacting with the bearing surfaces. This mechanism leads to cutting, blowing, and material removal. It was resulting in larger scar widths, particularly on the inner race. Conversely, soft contaminants, such as solid coal particles, primarily cause abrasive wear due to third-body abrasive, characterized by smoother but widespread discoloration due to increased temperature at a particle size of 250 μm and some flaxing occurring on the surface of the outer ring, resulting in starvation due to a lack of lubricant where the wear mechanism was fatigue wear. The same case occurs for other soft solid particles (limestone, gypsum, and clay).

The EDX analysis supports the wear mechanism by showing material transfer between solid contaminants and the ball and bearing on the outer race surfaces. This material exchange further exacerbates surface degradation and accelerates wear progression due to changes in the properties of the grease. From the EDX analysis, there were differences in the elemental composition of the material on the outer race surface before and after testing, as shown in Figs. 13 and 14, respectively. In general, the elemental composition of the material on the outer ring surface after testing is Fe, C, and O, and Cr. The elemental composition of O appears on the outer race surface as an indication of adhesion due to material transfer of solid contaminants and oxidation due to corrosion. The elemental composition of the Cr of the ball experienced adhesive wear on the surface of the outer race; the same thing was found by Demirsöz [20].

4.2 Monitoring of operational parameters as an indicator of wear mechanism on the surface of the outer and inner races

During the test, the vibration signal, temperature, and current were monitored in real time. The results of measurements of RMS vibration and temperature of bearings and current of the motor, as shown in Figs. 5, 6, 7, and 8, were strongly correlated with the presence of wear that occurred on the surfaces of the outer and inner races, as demonstrated in studies linking operational parameters to wear progression under contaminated conditions (e.g., Hariharan and Srinivasan [7]). The results of the average of RMS amplitude, temperature, and current are tabulated in Table 3. Vibration analysis of the bearings was carried out by installing an accelerometer sensor in the bearing housing, and the RMS acceleration amplitudes were obtained for several types of solid contaminants and particle sizes and without solid contaminant, as can be seen in Figs. 5 and 6, respectively. The RMS amplitude value can be used as a measure of the energy in a vibration signal and is used to detect the severity of a fault of the bearings. The RMS vibration amplitude increased due to instability from surface irregularities of the inner ring and outer ring caused by abrasive solid contaminant particles to promote the progression of wear. At a particle size of 74 μm, the change in the RMS amplitude of vibration is not too large when compared to a particle size of 250 μm. The RMS amplitude of vibration of clay solid contamination with a particle size of 74 μm gives the maximum amplitude value among other solid contaminants where there is an increase in amplitude. which is quite significant at the beginning, increases slightly fluctuatingly until it reaches a time of 4 hours. The wear that occurs due to the increase in the RMS vibration amplitude can be seen in the SEM images of the outer race surface (Fig. 13f), where the surface is irregular due to abrasive wear and fatigue wear. The same as for silica solid contaminant at a particle size of 250 μm, where the RMS amplitude of vibration increases linearly with time, the wear occurs on the outer race surface from the SEM image (Fig. 14c) showing severe wear on the surface due to abrasive and fatigue wear.

From the measurement of temperature as shown in Fig. 7, frictional heat generated by abrasive interactions between solid particles and the surface of the outer ring and inner ring increases lubricant degradation and exacerbates wear

mechanisms indicated by the increasing temperature of the bearings. Especially for coal solid contaminants, the temperature increases drastically in the first 50 minutes, and as time increases, the temperature increases slightly for both types of particles. Coal solid contaminant with a particle size of 74 μm gives a high bearing temperature; the smaller the particle size of the coal solid contaminant, the more it will cause the bearing temperature to increase; this can cause the coal to be easily burned. This is in accordance with research conducted by Ajrash et al. [21], with a particle size of coal <74 μm; the minimum auto-ignition temperature (MAIT) of coal is 235°C where the smaller the particle size of the coal, the lower the MAIT will be. Unlike hard solid contaminants such as silica and iron sand, abrasive wear due to hard particles causes a significant increase in bearing temperature but is still below the temperature of coal solid contaminants. The increase in temperature that occurs in the bearing is not influenced by the hardness of the solid contaminant but is more influenced by the type of solid contaminant. Ductile or soft materials are more likely to cause high bearing temperatures because there is high friction in the contact area, the same thing found by Nikas et al. [12].

Table 3. The average of RMS amplitude, temperature, and current with different contaminants and sizes.

Solid conta-minat	Size, μm	The average RMS amplitude, g	The average temperature, °C	The average current, Ampere
Without		2.92	60.81	2.67
Iron sand	74	3.93	68.39	2.53
	250	4.35	71.44	2.57
Coal	74	3.64	95.30	2.49
	250	5.13	82.66	2.60
Silica	74	3.67	69.09	2.55
	250	5.84	69,98	2.49
Lime-stone	74	3.71	78.26	2.66
	250	3.42	56.72	2.67
Gyp-sum	74	3.31	70.34	2.55
	250	3.61	75.05	2.67
Clay	74	4.95	59.82	2.61
	250	4.10	62.90	2.41

Indirect measurement of electric current in electric motors can be used to estimate the motor's torque. The amount of torque required by the motor to transmit power to the shaft to be driven depends on the amount of friction torque that occurs in the bearings. The amount of electric current measured in the motor with variations in solid contaminants in the bearings with two particle sizes can be seen in Figure 8. Higher resistance due to increased friction on the bearing reflects the increase in current in the motor as a result of the mechanical impact of two-body and third-body wear on the bearing operation. The largest motor current due to the presence of solid contaminants in the bearings for both types of particle sizes is caused by limestone solid contamination. The larger the particle size, the greater the value of the motor current. The effect of sticky soft particles, such as limestone trapped in the contact area, could provide resistance so that the current in the motor increases.

The lubricant regime of ball bearings is operated on an elastohydrodynamic lubrication (EHL) regime [11, 17]. In the EHL regime, the lubricant film thickness is smaller than 1 μm [22]. The solid contaminant sizes that are small or equal to the film thickness in the EHL regime will be entrapped in the contact area. When solid contaminant sizes larger than the oil film thickness enter the contact zone, they cause stress peaks and permanent indentations in the raceway as they are overrolled [2, 10]. Hard contaminants (iron sand and silica) act as cutting agents, removing material through abrasive wear, as detailed in studies exploring the dual mechanisms of wear caused by two-body and third-body interactions (e.g., Koulocheris et al. [2]; Hamilton et al. [5]) through material transfer and deformation. This duality underscores the critical role of contaminant properties in determining wear severity. While softer contaminants (clay, limestone, gypsum, and coal) induce third-body wear, they can change the physical properties of the grease lubricant, causing the contact surfaces to

lack lubrication, triggering starvation phenomena. Most soft solid contaminants trigger fatigue wear. According to Maru et al. [10] and Nikas et al. [12], the particles entrapped in the contact zone are causing local oil starvation, increased heating, and material melting. Flammable solid contaminants such as coal, as the surface friction increases over time, can increase the temperature, causing the coal to burn easily. This can be seen on the contact surface changing color due to the presence of solid particles from burning coal. From EDX analysis, adhesive wear occurs more dominantly on hard solid contaminants when compared to soft solid contaminants. This can be seen in Figure 13, where the elemental composition of the Cr material is higher. Addressing abrasive, adhesive, and fatigue wear on the bearings requires robust strategies, including advanced sealing systems to minimize contaminant ingress, high-performance lubricants capable of dispersing contaminants, and real-time monitoring of operational parameters to detect early signs of wear.

5. CONCLUSION

This study provides significant insights into the complex interplay between solid contaminant properties, surface morphology, and condition monitoring of bearing and motor regarding the wear pattern on the surface of the outer and inner rings. The findings can be summarized as follows:

1. Hard contaminants, such as silica and iron sand, predominantly induce abrasive wear through the two-body and third-body wear mechanism, resulting in scuffing, dents, and significant material removal. While soft contaminants, such as coal, primarily cause third-body wear mechanisms with smoother scars and flakes on the surface of the outer race due to decreasing the quality of lubricant and triggering starvation.
2. Scar width measurements, SEM and EDX analysis confirm the role of two-body wear and third-body wear in accelerating wear progression through cutting, plowing, and material transfer.
3. Monitoring the vibration, temperature, and current of the bearing and motor correlates strongly with the severity of wear, highlighting their importance as predictive maintenance indicators.
4. By incorporating the concept of monitoring operational parameters and wear mechanisms through wear patterns on the surface of inner and outer races, this study enhances our understanding of bearing damage and offers practical solutions to mitigate wear in contaminant-laden environments.

Acknowledgement

The paper is a part of the research done within the project Faculty of Engineering Y2025/2026. The authors would like to thank the Faculty of Engineering, Universitas Andalas.

REFERENCES

[1] M. Tomimoto, "Experimental verification of a particle induced friction model in journal bearings," *Wear*, vol. 254, no. 7–8, pp. 749–762, Apr. 2003, doi: 10.1016/s0043-1648(03)00250-3.

[2] D. Koulocheris, A. Stathis, Th. Costopoulos, and D. Tsantiotis, "Experimental study of the impact of grease particle contaminants on wear and fatigue life of ball bearings," *Engineering Failure Analysis*, vol. 39, pp. 164–180, Feb. 2014, doi: 10.1016/j.engfailanal.2014.01.016.

[3] T.-N. Ta, J.-H. Horng, M.-W. Huang, E. V. Torskaya, and C.-W. Kuo, "Tribological Characteristics and Vibration Response of Grease Lubricated Contacts under Environmental Particles and Water Impact," *Wear*, vol. 550–551, p. 205403, May 2024, doi: 10.1016/j.wear.2024.205403.

[4] J.-H. Horng, C.-C. Yu, and Y.-Y. Chen, "Effect of Third-Particle material and contact mode on tribology contact characteristics at interface," *Lubricants*, vol. 11, no. 4, p. 184, Apr. 2023, doi: 10.3390/lubricants11040184.

[5] R. W. Hamilton, R. S. Sayles, and E. Ioannides, "Wear due to debris particles in rolling bearing contacts," in *Tribology series*, 1998, pp. 87–93. doi: 10.1016/s0167-8922(98)80064-3.

[6] H. Boucherit, B. Bou-Saïd, and M. Lahmar, "The effect solid particle lubricant contamination on the dynamic behavior of compliant journal bearings," *Lubrication Science*, vol. 29, no. 7, pp. 425–439, Mar. 2017, doi: 10.1002/ls.1378.

[7] V. Hariharan and P. S. S. Srinivasan, "Condition monitoring studies on ball bearings considering solid contaminants in the lubricant," *Proceedings of the Institution of Mechanical Engineers Part C Journal of Mechanical Engineering Science*, vol. 224, no. 8, pp. 1727–1748, Jan. 2010, doi: 10.1243/09544062jmes1885.

[8] K. a. I. Sheriff, V. Hariharan, and B. Varunesh, "Performance Analysis of Ball Bearing with Solid Contaminants Using Vibration Analysis," in *Lecture notes in mechanical engineering*, 2021, pp. 175–182. doi: 10.1007/978-981-15-9809-8_14.

[9] K. A. I. Sheriff, V. Hariharan, and T. Kannan, "Analysis of solid contamination in ball bearing through acoustic emission signals," *Archives of Metallurgy and Materials*, vol. 62, no. 3, pp. 1871–1874, Sep. 2017, doi: 10.1515/amm-2017-0283.

[10] M. M. Maru, R. S. Castillo, and L. R. Padovese, "Study of solid contamination in ball bearings through vibration and wear analyses," *Tribology International*, vol. 40, no. 3, pp. 433–440, Jun. 2006, doi: 10.1016/j.triboint.2006.04.007.

[11] R. S. Dwyer-Joyce, "Predicting the abrasive wear of ball bearings by lubricant debris," *Wear*, vol. 233–235, pp. 692–701, Dec. 1999, doi: 10.1016/s0043-1648(99)00184-2.

[12] G. K. Nikas, R. S. Sayles, and E. Loannides, "Effects of debris particles in sliding/rolling elastohydrodynamic contacts," *Proceedings of the Institution of Mechanical Engineers Part J Journal of Engineering Tribology*, vol. 212, no. 5, pp. 333–343, May 1998, doi: 10.1243/1350650981542146.

[13] J.-H. Horng, T.-N. Ta, C.-W. Kuo, S.-J. Liao, and Y.-Y. Chen, "Development of Wear and Pitting Curves with Vibration Analysis for Lubricating Grease under Contamination Conditions," *Wear*, vol. 560–561, p. 205625, Nov. 2024, doi: 10.1016/j.wear.2024.205625.

[14] M. J. Ajrash, J. Zanganeh, and B. Moghtaderi, "Experimental investigation of the minimum auto-ignition temperature (MAIT) of the coal dust layer in a hot and humid environment," *Fire Safety Journal*, vol. 82, pp. 12–22, Mar. 2016, doi: 10.1016/j.firesaf.2016.02.007.

[15] J. Taha-Tijerina, B. Castaños-Guitrón, L. Peña-Parás, M. Tovar-Padilla, J. Alvarez-Quintana, and D. Maldonado-Cortés, "Impact of silicate contaminants on tribological and thermal transport performance of greases," *Wear*, vol. 426–427, pp. 862–867, Apr. 2019, doi: 10.1016/j.wear.2019.01.122.

[16] "TOP I Oil. Synthetic Hi-Temp Grease," Sep. 2017. http://top1oil.com/wp-content/uploads/2019/02/GREASE.pdf (accessed Jan. 01, 2025).

[17] D. Gasni, I. H. Mulyadi, J. Affi, and A. Y. Miswar, "Investigation of wear mechanism of ball bearings lubricated by Bio-Lubricant," *International Journal of Technology*, vol. 8, no. 7, p. 1248, Dec. 2017, doi: 10.14716/ijtech.v8i7.688.

[18] A. Ikhsan, D. Gasni, and M. Rusli, "Effect of several types of solid contamination in grease on tribological characteristics of two surfaces in contacts," *AIP Conference Proceedings*, vol. 3223, p. 040007, Jan. 2025, doi: 10.1063/5.0243058.

[19] A. Ikhsan, D. Gasni, and M. Rusli, "Investigation of the coefficient of friction, wear, and surface morphology on a sliding contact area due to the large particle size of solid contaminants in grease," *International Journal of Abrasive Technology*, vol. 12, no. 4, pp. 313–334, Jan. 2024, doi: 10.1504/ijat.2024.145179.

[20] R. Demirsöz, "Wear Behavior of Bronze vs. 100Cr6 Friction Pairs under Different Lubrication Conditions for Bearing Applications," *Lubricants*, vol. 10, no. 9, p. 212, Sep. 2022, doi: 10.3390/lubricants10090212.

[21] M. K. W. Ibrahim, D. Gasni, and R. S. Dwyer-Joyce, "Profiling a Ball Bearing Oil Film with Ultrasonic Reflection," *Tribology Transactions*, vol. 55, no. 4, pp. 409–421, Mar. 2012, doi: 10.1080/10402004.2012.664836.

[22] D. Koulocheris, A. Stathis, Th. Costopoulos, and G. Gyparakis, "Comparative study of the impact of corundum particle contaminants size on wear and fatigue life of grease lubricated ball bearings," *Modern Mechanical Engineering*, vol. 03, no. 04, pp. 161–170, Jan. 2013, doi: 10.4236/mme.2013.34023.